Synthesis and transport properties of Sr_xNbO_3 ($0.75 \leq x \leq 0.90$)

Kazuyuki Isawa, Jun Sugiyama, Kiyotaka Matsuura, Ayumi Nozaki,* and H. Yamauchi
Superconductivity Research Laboratory, International Superconductivity Technology Center, 10-13 Shinonome 1-chome, Koto-ku, Tokyo 135, Japan
(Received 18 May 1992; revised manuscript received 31 August 1992)

Polycrystalline samples of Sr_xNbO_3 ($0.75 \leq x \leq 0.90$) have been successfully synthesized by a solid-state reaction technique using TiO as a reducing agent. Powder x-ray-diffraction analysis indicated that the samples with $x \geq 0.80$ were single phase of the cubic perovskite structure. Electrical resistivity of each sample exhibited metallic behavior at temperatures below 300 K. For the samples with $x < 0.90$, the magnetic susceptibility was nearly temperature independent (Pauli paramagnetic), while the sample with $x = 0.90$ showed a Curie-Weiss behavior. Since the thermoelectric power coefficient (S) was found to be negative for all the samples in the temperature range between 10 and 300 K, the dominant charge carriers in Sr_xNbO_3 ($0.75 \leq x \leq 0.90$) were thought to be electrons. On the contrary, the nonlinear temperature dependence of S indicated that electrons in Sr_xNbO_3 were not simply metallic but rather similar to those in amorphous metals.

I. INTRODUCTION

Since the discovery of high-temperature superconductivity (HTSC) in certain copper oxides,[1] numerous experimental studies have been made to search for new superconductors exhibiting high T_c's. The highest T_c of 130 K has been reported for the Tl 2:2:2:3 phase.[2] The main features of the HTSC materials[3] may be summarized as follows.

(i) Crystallography speaking, the unit cell includes CuO_2 sheets and various types of charge reservoir blocks.

(ii) The structure in the vicinity of a CuO_2 sheet is considered to be of a modified perovskite block.

(iii) HTSC usually occurs as a result of charge-carrier injection in the CuO_2 sheet.

(iv) In the parent compounds, that is, nondoped cuprates, the copper ions in the CuO_2 sheet are in the state of $(3d)^9$ with $S = \frac{1}{2}$.

It should be emphasized that oxides other than copper oxides, especially V and Nb oxides, have also been intensively studied in order to search for new superconductors.[4–7] In contrast to the $(3d)^9$ configuration for the HTSC copper oxides, these noncopper oxides have d^1 configurations such as $(3d)^1$ for V^{4+} and $(4d)^1$ for Nb^{4+}. Actually, there are several reports on the superconducting layered oxides Li_xNbO_2 ($T_c = 5.5$ K) (Ref. 6) and $(Sr_{1-x}R_x)Nb_2O_6$ (R = La, Ce, Pr, Nd, Gd, and Ho) ($T_c = 12$ K).[7] Hence Nb oxides can be candidates for parent materials for HTSC materials.

Among Nb oxides, Sr_xNbO_3 ($x < 1$) has a perovskite-related structure containing an array of NbO_6 octahedra. Therefore it is worthwhile to synthesize a series of Sr_xNbO_3 samples with different values of x and investigate their properties.

The Sr_xNbO_3 compounds were first synthesized in 1955 independently by Ridgley and Ward[8] and Krylov and Shiarnin.[9] They reported that the samples with $0.70 < x < 0.95$ were nearly single phase with a cubic perovskite structure. For the samples with $0.60 < x < 0.70$, both cubic perovskite-type and tetragonal tungsten-bronze-type phases coexisted.[10] However, to our knowledge, there have been little data reported concerning the electrical and magnetic properties of Sr_xNbO_3.

In this paper we report the syntheses of polycrystalline Sr_xNbO_3 ($0.75 \leq x \leq 0.90$) and their transport properties, including resistivity, magnetic susceptibility, and thermoelectric power.

II. EXPERIMENTAL DETAILS

Polycrystalline samples of Sr_xNbO_3 ($0.75 \leq x \leq 0.90$) were prepared by a solid-state reaction technique using reagent-grade SrO and Nb_2O_5 powders. Stoichiometric mixtures were pressed into rectangular bars of $2 \times 2 \times 20$ mm^3. Each bar was encapsulated in an evacuated silica tube. In order to prepare samples in reducing atmospheres, TiO powder was used as the reducing agent. We used a reagent-grade TiO powder (~99%): The total weight of the TiO powder put in a sample ampule was 1.4 times heavier than the sample weight. Encapsulated samples were fired at 1050 °C for 80–160 h. The microstructures of the samples were observed by use of a scanning electron microscope (SEM). The composition of each sample was checked by electron-probe microanalysis (EPMA). The crystal structure of the sample was characterized by powder x-ray-diffraction (XRD) analysis using Cu $K\alpha$ radiation. The electrical resistivity of the sample was measured by a dc four-probe method. The dc magnetic susceptibility was measured using a superconducting quantum interference device (SQUID) magnetometer applying a magnetic field of $H = 10$ kOe. The thermoelectric power was measured by a dc method in the temperature range between 10 and 300 K. The temperature gradient (ΔT) in the sample was measured using two pairs of copper-Constantan thermocouples. These thermocouples were attached by silver epoxy glue on the

sample. The magnitude of ΔT was kept at 0.3–0.4 K throughout the measurement. To eliminate the effects from the reference leads (Cu wires), the absolute thermoelectric power of Cu was subtracted from the measured thermoelectric voltage.

III. RESULTS AND DISCUSSION

Figures 1(a) and 1(b) schematically show the crystallographic structure of perovskite, ABO_3, and a view of Sr_xNbO_3 ($x<1$) along the [100] direction, respectively. The structure of the cubic unit cell has been reported:[8,9] Sr atoms (at the A site in the regular perovskite structure) are randomly absent [as demonstrated in Fig. 1(b)], as in the tungsten bronzes or ReO_3.

EPMA measurements indicated that the distributions of both Sr and Nb were homogeneous in all the samples. According to SEM observations, all the samples were relatively porous. Figure 2 shows powder XRD patterns for the samples for $x=0.75$, 0.80, 0.85, and 0.90. Most of the diffraction lines were assigned to a cubic unit cell with the lattice constant $a\approx 0.4$ nm. Note that the diffraction pattern for the $Sr_{0.75}NbO_3$ sample included peaks due to unknown impurities besides those for the cubic phase. Also, the samples with $x=0.70$ and 0.95 were not single phase. Figure 3 shows the lattice constant a with respect to the Sr content x. The linear relationship between a and x indicates that the occupancy of the A site increases with increasing x.

The temperature dependence of electrical resistivity (ρ) is shown in Fig. 4 for the Sr_xNbO_3 samples with $0.75\le x\le 0.90$. The ρ-vs-T curves are more or less similar for all the samples except for one where $x=0.90$. That is, for the samples where $x<0.90$, ρ decreased monotonically with decreasing temperature. This is in good agreement with the previous ρ-vs-T data.[11] In Fig. 4 it is also seen that the sample gets more resistive as x approaches 0.90. For the sample with $x=0.90$, a broad maximum is seen for the ρ-vs-T curve at $\sim$200 K. However, the existence of this maximum must be reexamined since the present sample was polycrystalline and porous. That is, an artifact of a poorer pellet density may cause an increase of the absolute value of ρ.

The oxygen contents of the samples were determined by thermogravimetric measurements. The results showed that the oxygen deficiency (δ) for every sample was nearly zero ($\delta=0$). Thus the average Nb valencies for the samples with $x=0.75$, 0.80, 0.85, and 0.90 are expected to be 4.5, 4.4, 4.3, and 4.2, respectively. Note that the carrier concentration is expected to increase with increasing x. Nonetheless, all the samples with $x\le 0.90$ exhibited rather similar temperature dependences of ρ.

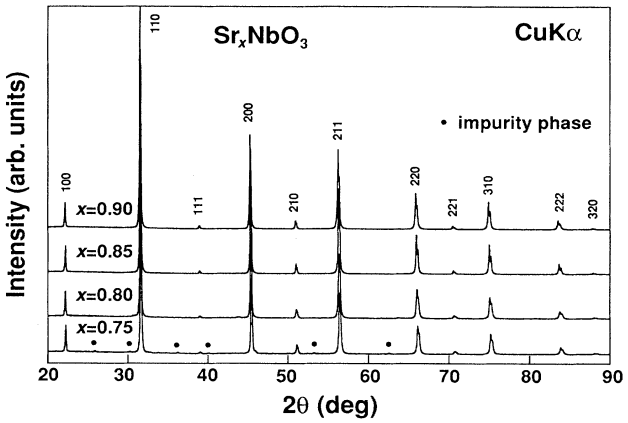

FIG. 2. Powder XRD patterns for Sr_xNbO_3 samples with $x=0.75$–0.90. Impurity peaks are marked with solid circles.

The temperature dependence of the dc magnetic susceptibility (χ) is shown in Fig. 5(a). For the samples with $x<0.90$, χ was nearly independent of temperature (Pauli paramagnetic) above 50 K, and below 50 K it slightly increased with decreasing temperature. The latter is suspected to be due to certain magnetic impurities, such as NbO_x,[12] which were not detectable by XRD analysis. Assuming that NbO_x impurities were included in the samples with $x<0.90$, the volume fractions of NbO_x may be estimated at $\sim$4% using the data of Cava *et al.* for NbO_x.[12] On the other hand, the $Sr_{0.90}NbO_3$ sample showed a Curie-Weiss behavior. This was thought not to be due to magnetic-impurity effects, but to an intrinsic property of the sample, since the magnitude of χ was one order of magnitude larger than those of χ's for the samples with $x<0.90$.

The χ-vs-T curve for the sample with $x=0.90$ is reproduced in Fig. 5(b) to make a curve fitting according to the Curie-Weiss relation

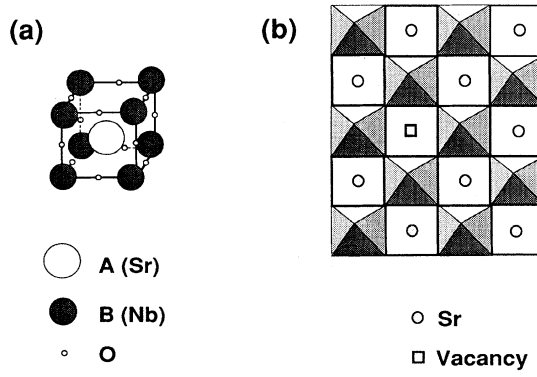

FIG. 1. (a) Schematic representation of perovskite structure. (b) (100) projection of Sr_xNbO_3 ($x<1$) structure. Sr vacancies (□) are randomly distributed.

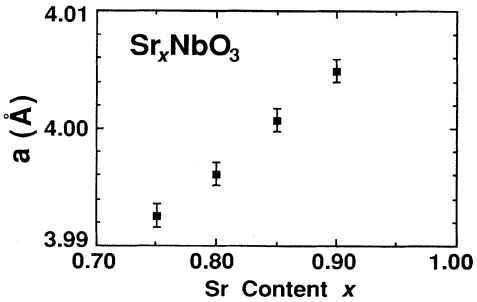

FIG. 3. Relationship between the lattice constant a and Sr content x.

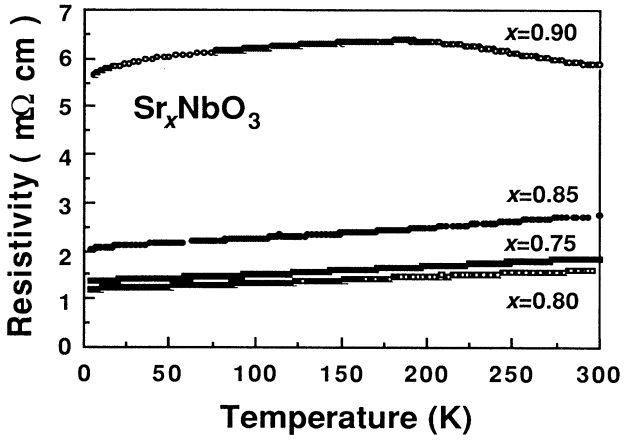

FIG. 4. Temperature dependence of electrical resistivity for Sr_xNbO_3. A broad maximum was observed for the sample with $x=0.90$ at a temperature around 200 K.

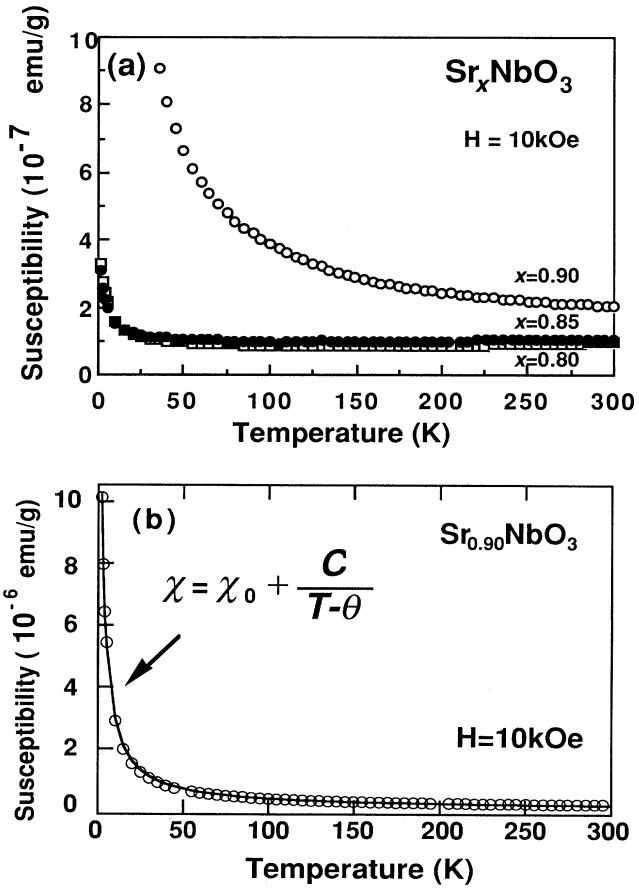

FIG. 5. (a) Temperature dependences of the magnetic susceptibility χ for Sr_xNbO_3 with $x=0.80$, 0.85, and 0.90. The data for $Sr_{0.75}NbO_3$ were similar to those for the samples with $x=0.80$ and 0.85. (b) Temperature dependence of the magnetic susceptibility for $Sr_{0.90}NbO_3$; the solid line represents a fitted curve using the Curie-Weiss relation [Eq. (1)] with $\chi_0=7.3\times10^{-8}$ emu/g, $C=3.3\times10^{-5}$ emu K/g, and $\Theta=1.2$ K.

$$\chi=\chi_0+\frac{C}{(T-\Theta)}\ , \tag{1}$$

in which χ_0 is a constant which is independent of temperature, C is a Curie constant, and Θ is an asymptotic Curie temperature. The fitted curve is for the parameters $\chi_0=7.3\times10^{-8}$ emu/g, $C=3.3\times10^{-5}$ emu K/g, and $\Theta=1.2$ K. Only if the Nb^{4+} ions are responsible to the magnetic moment can we calculate an effective magnetic moment $\mu_{\rm eff}$ using the formula

$$C=\frac{N_m\mu_{\rm eff}^2}{3k_B}\ , \tag{2}$$

where N_m is the number of magnetic ions per unit volume and k_B is the Boltzmann constant. The value obtained for $\mu_{\rm eff}$ was $0.24\mu_B$ (where μ_B is the Bohr magneton), which was rather small compared with the value for a free Nb^{4+} ion, i.e., $1.73\mu_B$. Since the ρ-vs-T curve for $Sr_{0.90}NbO_3$ showed a metallic behavior, its magnetic property was expected to be Pauli paramagnetic. Contrary to this expectation, a Curie-Weiss behavior was obtained for the same sample. This Curie-Weiss behavior may be caused by the following possible origins: (i) a characteristic electronic structure (narrow band), (ii) inequivalent sites for Nb ions, and/or (iii) stacking faults.

(i) Characteristic electronic structure: A metal with a wide band is ordinarily Pauli paramagnetic, while the χ-vs-T curve of a narrow-band system shows a Curie-Weiss behavior.[13] The conduction band of Sr_xNbO_3 is considered to be caused by the hybridization between the Nb $4d$ and O $2p$ orbitals, being similar to the case of tungsten-bronze compounds.[14] If the band structure changed at around $x=0.90$, we may attribute the Curie-Weiss behavior to this. A more detailed investigation of the electronic structure of this sample is required.

(ii) Inequivalent sites for Nb ions: The random Sr vacancies may yield inequivalent sites for Nb ions, as proposed for $Nb_{12}O_{29}$ by Cava *et al.*[12] In such a situation, Nb ions located at some sites may be localized, while those at other sites may remain in a delocalized state.

(iii) Stacking faults: Stacking faults or lattice imperfections in a crystal generally exhibit a Curie-Weiss contribution.[15]

Figure 6(a) shows the temperature dependence of thermoelectric power (S) for the samples with $0.75\le x\le0.90$. S's for all the samples are found to be negative in the temperature range between 10 and 300 K. Therefore the dominant charge carriers are thought to be electrons. As the temperature is lowered, S increased from ~-20 to ~-2 μV/K and dS/dT for every sample decreased with temperature. It is worth noting that the value of dS/dT for $Sr_{0.90}NbO_3$ was the smallest.

The total thermoelectric power (S) is usually expressed by the sum of three contributions,

$$S=S_d+S_p+S_m\ , \tag{3}$$

where S_d is the term for thermal diffusion, S_p for the phonon drag, and S_m for the magnon drag of conduction electrons. To the zeroth-order approximation, the three contributions are thought to be independent of each oth-

er. It is known that the peak of $|S_p|$ is observed in the temperature range between $\Theta_D/10$ and $\Theta_D/5$,[16] where Θ_D is the Debye temperature. To our knowledge the value of Θ_D for Sr_xNbO_3 is unknown. For Eu_xNbO_3, whose crystal structure is the same as that for Sr_xNbO_3, Θ_D has been estimated to be 343 K.[17] Nevertheless, no peaks for phonon drag were observed at temperatures below 300 K. This may be because the phonon drag was suppressed by a certain disorder such as that in the Sr occupancy.[18] Furthermore, the contribution S_m may be ignored, because any significant magnetic orders have not been reported for Sr_xNbO_3. Therefore the S_d term is considered to be the predominant one in Eq. (3).

The following three models for S are worth discussing for an explanation of the nonlinear temperature dependence of S assuming that $S=S_d$.

(i) For metals with spherical Fermi surfaces, S_d is expressed by the Mott formula[19]

$$S_d \propto T/E_F \ , \tag{4}$$

where E_F is the Fermi energy. By this model the nonlinear dependence of S on T cannot be explained unless the shape of the Fermi surface is dependent on T.

(ii) For semiconductors in which conduction occurs as a result of electron variable-range hopping between localized states in the energy gap, S_d is expressed as[18,19]

$$S_d \propto T+\beta T^{1/2} \ , \tag{5}$$

where $\beta T^{1/2}$ is the hopping term with β being a constant. Figure 6(b) shows a fitted curve based on Eq. (5) (with $\beta \sim 25$ $K^{1/2}$). Although the fitting seems to be in good agreement with the experimental data for the sample with $x=0.90$, no evidence for variable-range hopping is seen in the ρ-vs-T curve given in Fig. 4.

(iii) For metals in which electron-phonon interactions play a significant role for S at low temperatures, S_d is given as[20,21]

$$S_d = S_0[1+\alpha\lambda(T)]T \ , \tag{6}$$

where $\lambda(T)$ is the temperature-dependent enhancement of S due to electron-phonon interactions, S_0 is the bare thermoelectric power, and the coefficient α is approximately equal to unity, if additional effects are negligible.[21] The experimental data of S for glassy metals[22] and amorphous films[23] provided evidence that the electron-phonon enhancement was the dominant factor for nonlinear S-vs-T curves. Since there are randomly distributed vacancies on Sr sites in Sr_xNbO_3, we may consider that Sr_xNbO_3 is similar to the case of amorphous metals in terms of the transport property. Then Eq. (6) is considered to be a reasonably good expression for the nonlinear S-vs-T curve.

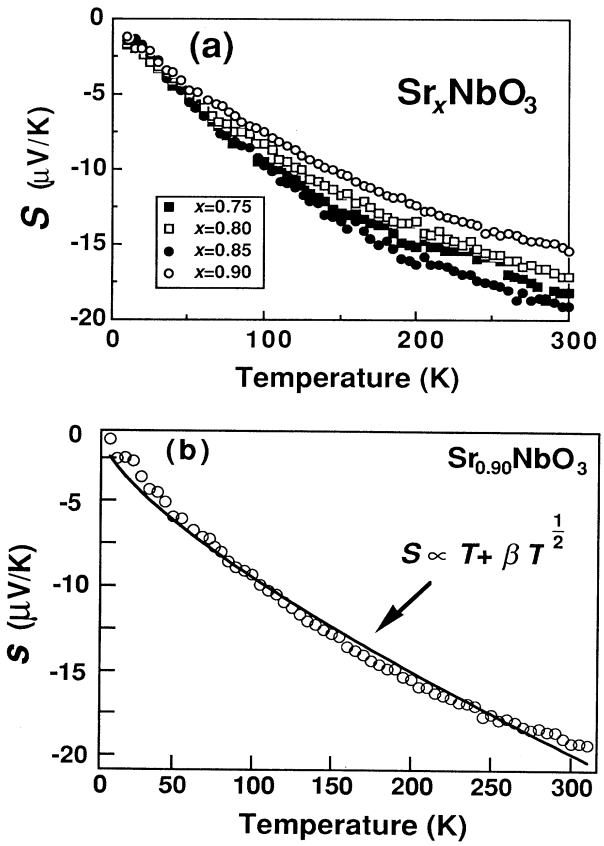

FIG. 6. (a) Temperature dependence of thermoelectric power for Sr_xNbO_3 ($0.75 \le x \le 0.90$). (b) The relationship between thermoelectric power and temperature for $Sr_{0.90}NbO_3$. The solid line represents the fitted curve using Eq. (5) with $\beta \sim 25$ $K^{1/2}$.

IV. SUMMARY

Polycrystalline samples of Sr_xNbO_3 ($0.75 \le x \le 0.90$) were successfully synthesized by a gettering technique using titanium mono-oxide as the reducing agent. Powder x-ray-diffraction analysis indicated that the samples with $x \ge 0.80$ were single phase of a cubic perovskite structure. From the electrical-resistivity data, every sample exhibited metallic behavior at temperatures below 300 K, though, as x increased, the sample became more resistive. For the samples with $x < 0.90$, the magnetic susceptibility was nearly temperature independent (Pauli paramagnetic), though the sample with $x=0.90$ exhibited a Curie-Weiss behavior. Since thermoelectric power coefficients (S) were found to be negative for all the samples in the temperature (T) range between 10 and 300 K, the dominant charge carriers were thought to be electrons. It was found that the relationship between S and T was nonlinear. A particular electron-phonon interaction was thought to be the dominant factor for this nonlinearity, as previously proposed for glassy metals and/or amorphous-metal films.

ACKNOWLEDGMENTS

The authors would like to thank J. Devemy of Ecole Europeenne des Hautes Etudes des Industries Chimiques

de Strasbourg for his help in sample preparation and K. Yamamoto and S. Takano of SRL-ISTEC for their kind help in SEM and EPMA analyses. We are also indebted to Dr. R. Itti, K. Kubo, and M. Kosuge of SRL-ISTEC for their helpful discussions. This work was supported by the New Energy and Industrial Technology Development Organization in the program for R&D Basic Technology for the Future Industries.

*Present address: Materials & Electronic Device Laboratory, Mitsubishi Electric Corp., 1-57, Miyashimo 1-chome, Sagamihara-shi, Kanagawa-ken 229, Japan.

[1]J. G. Bednorz and K. A. Müller, Z. Phys. B **64**, 189 (1986).
[2]T. Kaneko, H. Yamauchi, and S. Tanaka, Physica C **178**, 337 (1991).
[3]K. Yvon and M. Francois, Z. Phys. B **76**, 413 (1989).
[4]A. Nozaki, H. Yoshikawa, T. Wada, H. Yamauchi, and S. Tanaka, Phys. Rev. B **43**, 181 (1991).
[5]R. J. Cava, B. Batlogg, J. J. Krajewski, P. Gammel, H. F. Poulsen, W. F. Peck, Jr., and L. W. Rupp, Jr., Nature (London) **350**, 598 (1991).
[6]M. J. Geselbracht, T. J. Richardson, and A. M. Stacy, Nature (London) **345**, 324 (1990).
[7]J. Akimitsu, J. Amano, H. Sawa, O. Nagase, K. Gyoda, and M. Kogai, Jpn. J. Appl. Phys. **30**, L1155 (1991).
[8]D. Ridgley and R. Ward, J. Am. Chem. Soc. **77**, 6132 (1955).
[9]E. I. Krylov and A. A. Shiarnin, J. Gen. Chem. USSR **25**, 1637 (1955).
[10]N. Nguyen, J. Choisnet, and B. Raveau, C. R. Acad. Sci. Paris C **282**, 303 (1976).
[11]B. Hessen, S. A. Sunshine, T. Siegrst, and R. Jimenez, Mater. Res. Bull. **26**, 85 (1991).
[12]R. J. Cava, B. Batlogg, J. J. Krajewski, H. F. Poulsen, P. Gammel, W. F. Peck, Jr., and L. W. Rupp, Jr., Phys. Rev. B **44**, 6973 (1991).
[13]T. Moriya, in *Electron Correlation and Magnetism in Narrow-Band Systems,* edited by T. Moriya (Springer-Verlag, Tokyo, 1981), pp. 2–28.
[14]J. B. Goodenough, in *Progress in Solid State Chemistry,* edited by H. Reiss (Pergamon, Oxford, 1971), Vol. 5, pp. 145–399.
[15]T. Tsuda, *Electronic Conduction in Oxides* (Springer-Verlag, Tokyo, 1991).
[16]R. D. Barnard, *Thermoelectricity in Metals and Alloys* (Taylor & Francis, London, 1972), pp. 113–156.
[17]K. Ishikawa, G. Adachi, M. Hasegawa, K. Sato, and J. Shiokawa, J. Electrochem. Soc. **128**, 1374 (1981).
[18]A. B. Kaiser, Phys. Rev. B **40**, 2806 (1989).
[19]N. F. Mott, *Conduction in Non-Crystalline Materials* (Oxford, London, 1987).
[20]A. B. Kaiser, A. L. Christie, and B. L. Gallagher, Aust. J. Phys. **39**, 909 (1986).
[21]A. B. Kaiser and C. Uher, in *Studies of High Temperature Superconductors,* edited by A. V. Narlikar (Nova Science, New York, 1990), Vol. 7, pp. 16–24.
[22]B. L. Gallagher and B. L. Hickey, J. Phys. F **15**, 911 (1985).
[23]K. D. D. Rathnayaka, A. B. Kaiser, and H. J. Trodahl, J. Phys. F **15**, 921 (1985).